Growth of a single stripe and a stripe phase from individual holes in the low-doping regime of a strongly correlated electron system

Fan Yang[1,*] and Su-peng Kou[2,3]
[1]*Department of Physics, Beijing Institute of Technology, Beijing, 100081, China*
[2]*Center for Advanced Study, Tsinghua University, Beijing, 100084, China*
[3]*Department of Physics, Beijing Normal University, Beijing, 100874, China*
(Received 20 June 2004; revised manuscript received 7 February 2005; published 31 August 2005)

In this paper, it is shown how a single stripe and a stripe phase grow from individual holes in the low-doping regime. In an effective low-energy description of the *t-J* model, i.e., the phase-string model, a hole doped into the spin-ordered phase will induce a dipolar distortion in the background [Kou and Weng, Phys. Rev. B **67**, 115103 (2003)]. We analyze the hole-dipole configurations with lowest energy under a dipole-dipole interaction and show that these holes tend to arrange themselves into a regular polygon. Such a stable polygon configuration will turn into a stripe as the number of hole dipoles becomes thermodynamically large and eventually a uniform stripe state can be formed, which constitutes an energetically competitive phase at low doping. We also briefly discuss the effect of Zn impurities on individual hole dipoles and stripes.

DOI: 10.1103/PhysRevB.72.085134 PACS number(s): 71.27.+a, 71.10.−w

I. INTRODUCTION

The stripe phenomenon is one of many interesting properties observed in high-T_c cuprate superconductors. Static stripes were first experimentally found in $La_{1.48}Sr_{0.12}Nd_{0.4}CuO_4$ by neutron scattering,[1] where narrow elastic magnetic superlattice peaks located at $(\pi(1\pm 2x),\pi,0)$ and charge-order peaks at $(4\pi(1\pm x),0,0)$ are clearly identified at doping concentration $x=0.118$. This result is interpreted to mean that dopant-induced holes collect in the domain walls that separate antiferromagnetic (AF) antiphase domains. This picture is also supported by x-ray diffraction experiments.[2] In $La_{2-x}Sr_xCuO_4$ compounds, people have also tried to use dynamical stripes to explain the observations by inelastic neutron scattering,[3] where narrow magnetic peaks were found at the AF wave vectors $(\pi(1\pm\varepsilon),\pi,0)$ and $(\pi,\pi(1\pm\varepsilon),0)$ with $\varepsilon\sim 2x$ at low energies. Somewhat similar incommensurate dynamic magnetic fluctuations were also reported[4] in YBCO compounds. Nuclear quadruple resonance,[5] muon spin resonance,[6] and magnetic susceptibility measurements[7] all verify the evidence of stripe in $La_{2-x}Sr_xCuO_4$. Stripes have also been observed in oxygen-doped La_2CuO_4 using nuclear magnetic resonance techniques.[8] These experimental results suggest that the *stripe instability* may be extensively present in the cuprates as a competing order, which contributes to the complexity of the phase diagram.

The existence of stripes in a strongly correlated electron system was actually first predicted[9] by Zaanen and Gunnarsson *before* the experimental discovery. They found the stripe mean-field solution in a two-band Hubbard model, in which holes doped into the parent antiferromagnet generally tend to arrange themselves into straight lines aligned parallel to each other, i.e., charged stripes. Meanwhile, the stripe was also predicted in Refs. 10–17. Since the experimental discovery of static stripes in the cuprates, theoretical investigations of the stripe and stripe-related physics have been conducted very intensively in the high-T_c field. Numerical studies of the *t-J* model by the DMRG method present conflicting conclusions as to the existence of stripe phases in its ground state, which might be caused by the strong finite-size effects.[10] Recent theoretical developments in stripe physics have been reviewed in Refs. 11.

So far most theoretical studies on the origin of the stripes in the cuprates are either based on phenomenological theories or focused on the static ones at the mean-field level. To truly understand the microscopic origin of the stripe phase and its competitive relation with the homogeneous phases (including superconductivity), one needs to know when a stripe can be melted and broken into pieces, namely, what it is made of, and when it can become stable against various kinds of fluctuational effects.

Recently, it has been shown[18,19] that there exists a *more* stable elementary object, known as a hole dipole, in the low-doping spin-ordered phase described by the *t-J* model. Such a charge $+e$ entity can be regarded as a dipole composed of a charged vortex (centered at a spinless holon) and a neutral antivortex which is self-trapped in real space. Due to the so-called phase-string effect, an infinite (logarithmic divergent) energy is needed if one is to "destroy" such a composite by moving two poles of the dipole infinitely far apart.

On the other hand, since each hole dipole is self-trapped in real space, its kinetic energy is suppressed. Thus the potential energy (from impurities, for instance) and the dipole-dipole interaction between two holes will become dominant. In the absence of disorder or impurities and without considering the long-range Coulomb repulsion, an inhomogeneous instability has been found in such a system and in particular various stripe instabilities were suggested[19] to occur. In other words, if a stripe does form in this system, the hole dipoles described above will become the elementary building blocks. Consequently the fluctuations and dynamics of stripes as well as the melting of them may be understood and mathematically described based on the hole dipoles.

In this paper, we shall follow up the stripe instability pointed out in Ref. 19 and demonstrate mathematically how

a *stable* stripe can grow from individual hole dipoles by starting with only a few of them. We find that this finite number of hole dipoles generally forms a regular polygon with a minimized potential energy, which is stable against the perturbations. With the increase of the hole number, the polygon eventually evolves into a stripe and then stripes as the hole concentration becomes finite in the thermodynamic limit, which results in the stripe phase. We further consider Zn impurity effects on both hole dipoles and stripes and predict that stripes can be easily destroyed in the presence of random zinc atoms.

II. THE MODEL

A. The phase-string model

We start with the two-dimensional *t-J* model. At half filling, it turns into the Heisenberg model with a good description of the magnetic properties in cuprates. The Marshall sign rule is found[16] in the ground state of such a model, where the flips of two antiparallel spins at opposite sublattice sites are always accompanied by a sign change in the ground-state wave function: $\uparrow\downarrow \rightarrow (-1)\downarrow\uparrow$. Upon doping, however, this Marshall sign rule will get frustrated by the motion of the doped holes. When a hole hops from site to site, a sequence of ± signs will be left behind which cannot be repaired by spin-flip processes; it is called a phase string.[15]

The phase-string theory is developed to accurately handle the phase-string effect in the *t-J* model. This theory is based on a kind of slave-particle formula in which the electron operator reads[17]

$$c_{i\sigma} = h_i^{\dagger} b_{i\sigma} (-\sigma)^i e^{i\hat{\Theta}_{i\sigma}}, \tag{1}$$

where $h_i^{\dagger}$ is a bosonic "holon" creation operator and $b_{i\sigma}$ is a bosonic "spinon" annihilation operator, satisfying the following no-double-occupancy constraint:

$$h_i^{\dagger} h_i + \sum_{\sigma} b_{i\sigma}^{\dagger} b_{i\sigma} = 1. \tag{2}$$

Here the nonlocal phase factor $e^{i\hat{\Theta}_{i\sigma}}$ precisely keeps track of the singular part of the phase-string effect as well as the fermionic statistics of the electron operator, as defined by

$$e^{i\hat{\Theta}_{i\sigma}} = e^{(i/2)(\Phi_i^b - \sigma\Phi_i^h)}, \tag{3}$$

with

$$\Phi_i^b = \sum_{l\neq i} \mathrm{Im}\ln(z_i - z_l)\left(\sum_{\alpha} \alpha n_{l\alpha}^b - 1\right) \tag{4}$$

and

$$\Phi_i^h = \sum_{l\neq i} \mathrm{Im}\ln(z_i - z_l) n_l^h. \tag{5}$$

The effective phase-string model of the *t-J* Hamiltonian is given by

$$H_{\mathrm{eff}} = -t_h \sum_{\langle ij\rangle} \left[\left(e^{iA_{ij}^s}\right) h_i^{\dagger} h_j + \mathrm{H.c.}\right] - J_s \sum_{\langle ij\rangle\sigma} \left[\left(e^{i\sigma A_{ij}^h}\right) b_{i\sigma}^{\dagger} b_{j-\sigma}^{\dagger} + \mathrm{H.c.}\right], \tag{6}$$

with $t_h \sim t, J_s \sim J$. The most important and unique structure of the phase-string theory is the mutual dual relation in Eq. (6): For holons, a spinon simply behaves like a $\pm\pi$ flux tube and for spinons, a holon also behaves like a π flux tube, which are described by the lattice gauge fields A_{ij}^s and A_{ij}^h as follows:

$$\sum_C A_{ij}^s = \frac{1}{2} \sum_{\sigma, l\in C} (\sigma n_{l\sigma}^b) \tag{7}$$

and

$$\sum_C A_{ij}^h = \frac{1}{2} \sum_{l\in C} n_l^h \tag{8}$$

for a closed path C with $n_{l\sigma}^b$ and n_l^h denoting spinon and holon number operators, respectively.

B. Holes as dipoles

In the phase-string theory, the spin-flip operator is defined as

$$S_i^+ = (-1)^i b_{i\uparrow}^{\dagger} b_{i\downarrow} \exp\left[i\Phi_i^h\right] \tag{9}$$

with

$$\Phi_i^h = \sum_{l\neq i} \mathrm{Im}\ln(z_i - z_l) n_l^h. \tag{10}$$

In the AF spin-ordered phase, the spinons are Bose condensed, i.e., $\langle b_{i\sigma}\rangle \neq 0$, with the spins lying in the *xy* plane. Experimentally, in the high-T_c cuprate superconductors, the spins almost lie in the Cu-O plane,[20] with a small canting angle away from the plane.[21] Theoretically, small anisotropic terms are added into the SU(2)-invariant Heisenberg Hamiltonian to fix the direction of the spins.[22] The polarization direction of the spin ordering is determined by $\langle S_i^+\rangle = (-1)^i \langle b_{i\uparrow}^{\dagger}\rangle \langle b_{i\downarrow}\rangle \exp[i\Phi_i^h]$. From this, we can see that besides the sign $(-1)^i$, which reflects the staggered AF order, there is an additional phase $\exp[i\Phi_i^h]$ introduced by holons, which represents a twist of the spins with respect to each holon; namely, each time one circles around a holon once, a 2π rotation is found in the direction of the spin ordering. The resulting spin configuration is called a meron (spinon vortex) (Fig. 2 of Ref. 19). A meron costs an energy that is logarithmically dependent on the size of the system. For two holons, the induced spin twists are in the same way such that there exists a repulsive interaction between them. In order to remove such an unphysical energy divergence, an antimeron should be induced[19] near every holon meron to cancel out the spin twists at large distance. An antimeron is defined by

$$b_{i\sigma} \rightarrow \tilde{b}_{i\sigma} \exp\left[i\frac{\sigma}{2}\vartheta_i^k\right], \tag{11}$$

where $\vartheta_i^k = \mathrm{Im}\ln(z_i - z_k^0)$. Here z_k^0 denotes the coordinate of the center of an antimeron labeled by k. As a result

$$\langle S_i^+ \rangle \to (-1)^i \langle \tilde{b}_{i\uparrow}^\dagger \rangle \langle \tilde{b}_{i\downarrow} \rangle \exp[i\Phi_i^h - i\vartheta_i^k]. \tag{12}$$

Define

$$\phi_i^k = \Phi_i^h - \vartheta_i^k = \mathrm{Im} \ln \frac{z_i - z_k/2}{z_i + z_k/2} \tag{13}$$

to describe the spin twist, with $z_k \equiv e_k^x + i e_k^y$. Here the meron and antimeron are centered at $\pm \mathbf{e}_k/2$, respectively. At $|\mathbf{r}_i| \gg |\mathbf{e}_k|$,, one obtains a dipolar twist

$$\phi_i^k \simeq \frac{(\hat{\mathbf{z}} \times \mathbf{e}_k) \cdot \mathbf{r}_i}{|\mathbf{r}_i|^2}. \tag{14}$$

The energy cost of such a dipole configuration is given as the following:[19]

$$\mathcal{E}_k^d \simeq \frac{J_s \rho_c^s a^2}{4} \int d^2\mathbf{r} \frac{|\mathbf{e}_k|^2}{|\mathbf{r} - \mathbf{e}_k/2|^2 |\mathbf{r} + \mathbf{e}_k/2|^2} \simeq q^2 \ln \frac{|\mathbf{e}_k| + a}{a},$$

$$q^2 = \pi J_s \rho_c^s a^2, \tag{15}$$

which is finite. In the above $\rho_c^s a^2 = \langle b^+ \rangle^2$ (a is the lattice constant). This meron-antimeron spin configuration is called a hole dipole.[18,19] The displacement connecting the centers of a meron and an antimeron can be defined as the dipole moment here. The dipole moment is determined by the two-dimensional Coulomb gas theory by a standard Kosterlitz-Thouless renormalization-group (RG) method.[18,19] Near half filling $x \to 0$ we estimate the centers of a meron and an antimeron as the lattice constant $\langle |\mathbf{e}_k| \rangle = r_0 \sim a$.

At the end of this part, we note that in somewhat different contexts, the concept of hole dipoles has also been suggested by different authors through different approaches. It is raised in Refs. 23,24 that the doped holes introduce a local ferromagnetic exchange coupling between their neighboring Cu^{2+} ions, which brings frustration to the background antiferromagnetism. The frustrating bond acts like a magnetic dipole. From this picture, these authors studied the suppression of antiferromagnetic correlations by the hole dipoles, and the magnetic phase diagram was obtained. It is also pointed out in Ref. 25 that doped holes in the form of a hole spin polaron interact with each other through a dipolar potential. It is just the excitation of these spin polarons that forms the stripe.[26,27] In Ref. 28, an analogy was given between the doped holes in an AF background with the ^{3}He impurity in the liquid ^{4}He. As a result, it is also found that a mobile hole creates a long-range dipolar spin backflow. And in Ref. 29, the interaction between the holes is more carefully considered, including the long-range Coulomb interaction, the dipolar potential, and the short-range attraction. The competing of these interactions leads to a complicated phase diagram, which includes a diagonal stripe. It should also be noticed that, beyond this local dipole picture, the physics of a few holes in the AF background was studied in other contexts which might lead to a ferron phase and phase-separation.

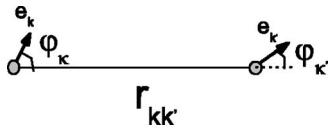

FIG. 1. The variables in formula (16) are shown. For two dipoles indexed by k and k', $r_{kk'}$ denotes the distance between their centers, e_k and $e_{k'}$ denote their moments, and φ_k and $\varphi_{k'}$ denote the angles between their moments and the line that connects their centers.

III. OPTIMAL CONFIGURATIONS FOR MULTIHOLE DIPOLES

A hole dipole is self-localized[19] in space with the suppression of its kinetic energy. If there is an impurity, such a hole dipole can be easily trapped around it, whose effect will be discussed in Sec. IV. In this section, we shall consider the impurity-free case, in which the hole dipole can be located anywhere in real space due to the translational symmetry. For multinumber hole dipoles, the dipole-dipole interaction will determine the in spatial configuration. In the following we start with the case of two hole dipoles first.

A. Energy-minimal configuration for two hole dipoles

For two dipoles well separated from each other, the interaction energy is given by[19]

$$\begin{aligned} V_{kk'}^{d\text{-}d} &\simeq \frac{2q^2}{|\mathbf{r}_{kk'}|^2} \left(\mathbf{e}_k \cdot \mathbf{e}_{k'} - 2 \frac{(\mathbf{e}_k \cdot \mathbf{r}_{kk'})(\mathbf{e}_{k'} \cdot \mathbf{r}_{kk'})}{|\mathbf{r}_{kk'}|^2} \right) \\ &= - \frac{2q^2 |\mathbf{e}_k| |\mathbf{e}_{k'}|}{|\mathbf{r}_{kk'}|^2} \cos(\varphi_k + \varphi_{k'}) \\ &\simeq - 2q^2 \frac{r_0^2}{|\mathbf{r}_{kk'}|^2} \cos(\varphi_k + \varphi_{k'}), \end{aligned} \tag{16}$$

in which the size of the dipoles is fixed by r_0. The alignments of the two dipoles are shown in Fig. 1.

Under the interaction (16), two dipoles will adjust their dipole moment directions to arrive at the lowest energy. It is easy to see that the condition to minimize their potential energy at a fixed distance is

$$\varphi_k + \varphi_k{}' = 0 \quad \text{modulo } 2\pi, \tag{17}$$

which results in an attractive potential energy,

$$V_1^{d\text{-}d} \sim - \frac{2q^2 r_0^2}{|\mathbf{r}_{kk'}|^2}. \tag{18}$$

Two dipoles will then move closer and closer until they reach a least distance $2r_0 = 2|\mathbf{e}_{k'}|$, determined essentially by the size of the dipoles. When the distance between two dipoles is near $2r_0$, the potential described by Eq. (16) usually is no longer correct. However, we shall use the formula (16) approximately at $|\mathbf{r}_{kk'}| \gtrsim 2r_0$ and take the positions of the dipoles as continuous variables by ignoring the discrete lattice sites in the following considerations of n-dipole case. Then the problem is reduced to a mathematical one to search for

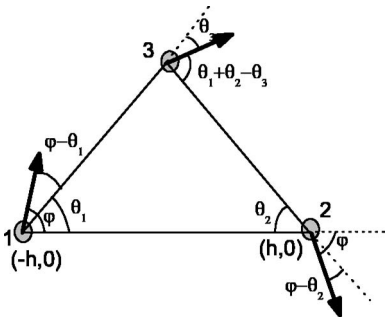

FIG. 2. Configuration for three dipoles marked by 1, 2, and 3. The arrows indicate the moments of the dipoles.

the optimum configuration for the n dipoles which interact with each other through (16), under the constraint that the distance between any two dipoles should be no less than twice the average dipole moment $|2\mathbf{e}_{k'}|=2r_0$.

B. Three and four hole dipoles

Now let us consider the three-dipole case. In Fig. 2, three hole dipoles are marked by 1, 2, and 3, respectively. Suppose the first and second dipoles are located at $(\pm h,0)$, with the angles between their dipole moments and the line connecting them $\pm\varphi$. Then we want to find out what is the optimal location for the third dipole. From Fig. 2, it is easy to see that for the dipoles marked by 1 and 3, one has

$$\varphi-\theta_1=\theta_3, \tag{19}$$

and for 2 and 3, one has

$$\varphi-\theta_2=\theta_1+\theta_2-\theta_3. \tag{20}$$

Then one finds

$$\varphi=\theta_2+\theta_1. \tag{21}$$

Defining the coordinate of the third dipole by (x,y), we get

$$\varphi=\arctan\left(\frac{y}{x+h}\right)+\arctan\left(\frac{y}{-x+h}\right), \tag{22}$$

and thus

$$\tan\varphi=\tan\left[\arctan\left(\frac{y}{x+h}\right)+\arctan\left(\frac{y}{-x+h}\right)\right]=\frac{-2hy}{x^2+y^2-h^2}, \tag{23}$$

such that

$$x^2+\left(y+\frac{h}{\tan\varphi}\right)^2=\frac{h^2}{\sin^2\varphi}. \tag{24}$$

From Eq. (24), we can see that the track of (x,y) is just a circle passing through dipoles 1 and 2, centered at $(0,-h/\tan\varphi)$ with a radius $R=h/\sin\varphi$. From knowledge of geometry, it is easy to see that the moments of these three dipoles will all point along the tangents of the circle, as shown in Fig. 3.

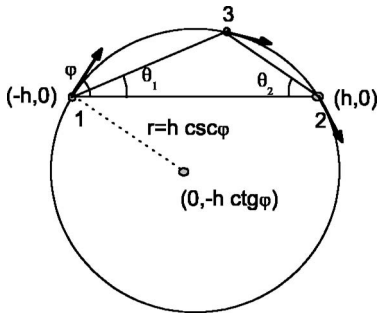

FIG. 3. For two dipoles 1 and 2 with their centers fixed at $(\pm h,0)$ and the angles between their moments and the line connecting their centers φ, the track of the center of dipole 3 to optimize the direction of its moment is a circle which passes the former two dipoles, centering at $(0,-h\cot\varphi)$, with the radius $h\csc\varphi$. The directions of the three dipoles are along the tangent of the circle.

Then the energy-minimal configuration for three hole dipoles is obtained as an equilateral triangle. The minimal interaction energy for three hole dipoles is

$$V_2^{d\text{-}d}\sim-3\times 2q^2\frac{r_0^2}{|\mathbf{r}_{kk'}|^2}=-2q^2\frac{r_0^2}{R^2}, \tag{25}$$

with $|r_{kk'}|=\sqrt{3}R$ and R the radius of the circle crossing the three dipoles.

When a fourth hole dipole is added, it should first make an optimal configuration with the dipoles 1 and 2, and thus is located on a circle as discussed above. Then by further making an optimal configuration with dipoles 1 and 3, it will also be located on another circle passing through the dipoles 1 and 3. Since the dipole 3 is already on a circle determined by 1 and 2, with its dipole moment along the tangent, the circle determined by the dipoles 1 and 3 is the same as that determined by the dipole 1 and 2, and so is the one determined by dipoles 2 and 3 (see Fig. 4).

The same argument is applicable to n dipoles. So the optimal configuration for n dipoles under the potential (16) will be always on a circle, with each dipole moment along the tangent of the circle and proportional spacing for each dipole. This configuration is just a regular polygon with n edges (see Fig. 5). At low energy the radius of the circle R

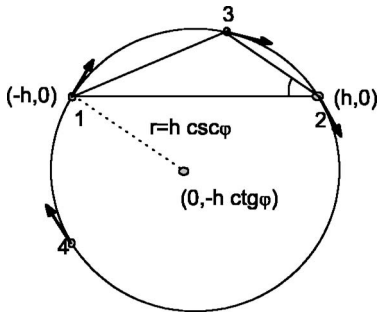

FIG. 4. When dipole 4 is added, it should make an optimum configuration with any two dipoles. As a result, it locates on the same circle mentioned in Fig. 3.

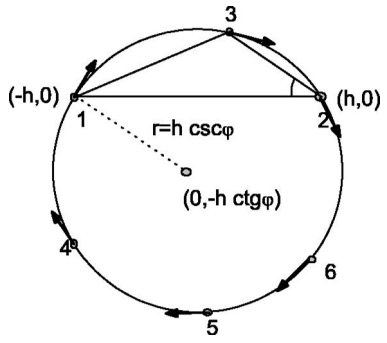

FIG. 5. When more dipoles are added, they should all locate on the circle mentioned in Figs. 3 and 4. Here $n=6$ is displayed.

will shrink until the length of every edge is equal to the minimum $2r_0$,.

$$R \simeq \frac{2r_0}{2\sin(\pi/n)} \tag{26}$$

The minimal interaction energy for n hole dipoles n is an odd number) is

$$V_n^{d\text{-}d} \sim -2q^2r_0^2\sum_{kk'}\frac{1}{|\mathbf{r}_{kk'}|^2} = -2q^2r_0^2 n \times 2 \times \sum_{k=1}^{(n-1)/2}\frac{1}{|\mathbf{r}_k|^2}, \tag{27}$$

with

$$|\mathbf{r}_k| = 2R\sin\left(\frac{\pi}{n}k\right) = 2r_0\frac{\sin(\pi k/n)}{\sin(\pi/n)}. \tag{28}$$

If n is an even number, the minimal interaction energy is

$$V_n^{d\text{-}d} \sim -2q^2r_0^2 n\left(2\sum_{k=1}^{n/2-1}\frac{1}{|\mathbf{r}_k|^2} + \frac{1}{2}\frac{1}{(2R)^2}\right). \tag{29}$$

Numerical simulations for up to $n=30$ dipoles also show that for these interacting dipoles, the optimized configurations with minimized total energy are always regular polygons as discussed above (see Fig. 6)

C. Stability of the regular polygon configuration

In this part we will show the stability of the regular polygon configuration for hole dipoles. For a regular polygon

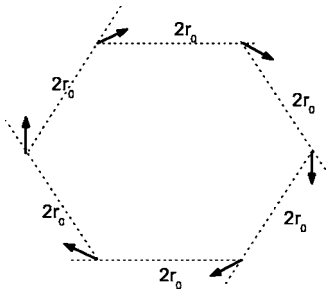

FIG. 6. The optimum configuration for n dipoles. Their centers form a regular polygon. The moment of each dipole is directed along the bisector of each external angle. Here $n=6$ is displayed.

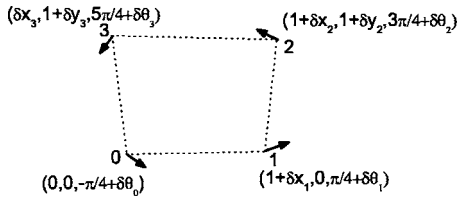

FIG. 7. A perturbation is imposed on the optimum configuration, i.e., the regular polygon. Here $n=2$ is displayed. Each dipole has a perturbation in the position and direction $(\delta x_i, \delta y_i, \delta\theta_i)$. The dipoles 0 and 1 are fixed at the origin point and on the x axis, respectively, as the total potential has global SO(2) invariance.

configuration, the distance between two nearest dipoles has reached the minimal $2r_0$. But the distances between other pairs of dipoles have not arrived at their minimum. Mathematically, it should be proved that the configuration is stable against perturbations.

1. Perturbation: Changing the direction of a dipole moment

First we change the direction of a dipole moment from its original direction φ_0 to $\varphi_0+\delta\varphi$. The change of the total energy for n hole dipoles n is an odd number) is

$$\Delta V^{d\text{-}d} \simeq -2q^2\sum_k \frac{r_0^2}{|\mathbf{r}_k|^2}[\cos(\varphi_0+\delta\varphi+\varphi_{k'}) - \cos(\varphi_0+\varphi_{k'})]$$
$$\simeq \left(q^2\sum_k \frac{r_0^2}{|\mathbf{r}_k|^2}\right)(\delta\varphi)^2, \tag{30}$$

with $|\mathbf{r}_k|$ defined by Eq. (28). On the other hand, if n is an even number, the energy difference is

$$\Delta V^{d\text{-}d} \sim q^2r_0^2\left(2\sum_{k=1}^{n/2-1}\frac{1}{|\mathbf{r}_k|^2} + \frac{1}{2}\frac{1}{(2R)^2}\right)(\delta\varphi)^2 > 0. \tag{31}$$

When more hole dipoles change the directions of their moments simultaneously, the energy cost is simply the sum of all the positive energy costs for every change.

So the regular polygon configuration is stable against changing the directions of the dipole moments $\Delta V^{d\text{-}d} > 0$.

2. Perturbation: Changing the positions of the centers of the dipoles

Next we change the positions of the centers of the dipoles. In Fig. 7, the case of $n=4$ is shown as an example. The position and direction of each dipole are marked in Fig. 7. Here $2r_0$ is set to be 1 for convenience. The dipoles 0 and 1 are fixed at the origin point and on the x axis, respectively. Each dipole has a perturbation in the position and direction $(\delta x_i, \delta y_i, \delta\theta_i)$. After this perturbation, we can expand the potential up to first order. Taking dipoles 1 and 2 as an example, we have

$$V_{12} = \frac{-V_0\cos(\varphi_1+\varphi_2)}{r_{12}^2}, \tag{32}$$

among which

$$V_0 = 2q^2 r_0^2. \tag{33}$$

For the numerator, we have

$$\varphi_1 + \varphi_2 = 0 + \delta\theta_1 + \delta\theta_2 - 2\delta\theta_{12}. \tag{34}$$

In the above equation, $\delta\theta_1$ and $\delta\theta_2$ denote the changes in the directions of the moments of dipoles 1 and 2, while $\delta\theta_{12}$ denotes the change in the direction of line connecting dipoles 1 and 2,

$$\delta\theta_{12} = \delta(x_1 - x_2)/1 = \delta x_1 - \delta x_2. \tag{35}$$

Thus the change in the numerator is zero to the first order of the perturbation. For the denominator, we have

$$\begin{aligned} r_{12}^2 &= (\delta x_1 - \delta x_2)^2 + (1 + \delta y_2)^2 \\ &= 1 + 2\delta y_2 + o(\delta x_1^2, \delta x_2^2, \delta x_1 \delta x_2). \end{aligned} \tag{36}$$

As a result, up to the first-order perturbation, the potential becomes

$$V_{12} = \frac{-V_0}{1 + 2\delta y_2} = -V_0 + 2V_0 \delta y_2 + o(\delta y_2^2). \tag{37}$$

In the same way, we expanded the potential among other dipoles, and obtained the following expansion of the total potential up to the first-order perturbation:

$$\begin{aligned} \delta V_{\text{tot}}^{d\text{-}d} &= \delta(V_{01} + V_{12} + V_{23} + V_{02} + V_{03} + V_{13}) \\ &= \frac{5}{2} V_0 (\delta x_1 + \delta x_2 - \delta x_3 + \delta y_2 + \delta y_3) \end{aligned} \tag{38}$$

To satisfy the constraint that the distances between the centers of any two dipoles should be no less than $2r_0$, we expanded the formula of their distances to the first-order perturbation and have

$$\begin{aligned} &\delta x_1 \geqslant 0 \rightarrow r_{01} \geqslant 1, \\ &\delta x_2 \geqslant \delta x_3 \rightarrow r_{23} \geqslant 1, \\ &\delta y_2 \geqslant 0 \rightarrow r_{12} \geqslant 1, \\ &\delta y_3 \geqslant 0 \rightarrow r_{03} \geqslant 1. \end{aligned} \tag{39}$$

From Eqs. (38) and (39), we obtained that

$$\delta V_{\text{tot}} \geqslant 0, \tag{40}$$

which denotes that the change of the total potential is not less than zero up to the first-order perturbation.

Our above demonstration can be easily generalized to arbitrary n. For a general n, we have

$$V_{\text{tot}} = \sum_{ij} \frac{-V_0 \cos(\varphi_i + \varphi_j)}{r_{ij}^2}. \tag{41}$$

Up to the first-order perturbation, we have

$$\delta V_{\text{tot}} = V_0 \sum_{ij} \frac{2(x_i - x_j)(\delta x_i - \delta x_j) + 2(y_i - y_j)(\delta y_i - \delta y_j)}{r_{ij}^4}. \tag{42}$$

The constraint for the least distance between any two adjacent dipoles reads

$$\begin{aligned} \delta r_{i,i+1} &= 2(x_i - x_{i+1})(\delta x_i - \delta x_{i+1}) \\ &\quad + 2(y_i - y_{i+1})(\delta y_i - \delta y_{i+1}) \geqslant 0. \end{aligned} \tag{43}$$

It can be checked that

$$\delta V_{\text{tot}} = g V_0 \sum_i \delta r_{i,i+1}, \tag{44}$$

in which

$$g = \frac{\sum_{i=2}^{n-1} \sin[\pi(i-1)/n]/[\sin(\pi i)/n]^3}{8 \sin(\pi/n)\sin(2\pi/n)} > 0. \tag{45}$$

From Eqs. (43)–(45), we have

$$\delta V_{\text{tot}} \geqslant 0. \tag{46}$$

From Eq. (46), we know that the change of the total potential is no less than zero up to the first-order perturbation for arbitrary n. When all the δx_i and δy_i are carefully chosen so that the equality is realized in Eqs. (43) and (46) turns into

$$\delta V_{\text{tot}} = 0. \tag{47}$$

In such cases, we should have to check the second-order perturbation in the potential energy as the first-order perturbation is zero. We again give our proof for $n=4$ as an example.

When $\delta x_1 = \delta y_2 = \delta y_3 = 0$ and $\delta x_2 = \delta x_3 = \delta x$, the equality is realized in Eq. (39) and hence in Eq. (40). The first-order perturbation of the total potential is zero, so we expanded it to the second-order perturbation, and obtained

$$\begin{aligned} V_{tol} &\geqslant \sum_{i,j} \frac{-V_0}{r_{ij}^2} \\ &= -2V_0 - \frac{2V_0}{1 + (\delta x)^2} - \frac{V_0}{1 + (1 - \delta x)^2} - \frac{V_0}{1 + (1 + \delta x)^2} \\ &= -5V_0 + \frac{3}{2} V_0 (\delta x)^2 + o((\delta x)^3), \end{aligned} \tag{48}$$

and therefore

$$\delta V_{\text{tot}} \geqslant \frac{3}{2} V_0 (\delta x)^2 \geqslant 0. \tag{49}$$

So the change in the total potential is also not less than zero up to the second-order perturbation.

In the case of $n > 4$, we can carry out a similar expansion, and draw the same conclusion.

By the above perturbative expansion, we proved that the configuration shown in Fig. 6 is stable against local perturbation in the positions and directions of the dipole moments.

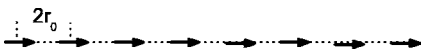

FIG. 8. When $n \to \infty$, the regular polygon shown in Fig. 6 turns into a line. The distance between the centers of neighboring dipoles is $2r_0$.

D. Energetically minimized configurations for infinite-number hole dipoles: Stripes

In the above part, we have proved that n dipoles will arrange themselves to form a regular polygon to minimize the energy. And the radius of the circle R will shrink until the length of every edge is equal to the minimum $2r_0$. When $n \to \infty$, the radius of the circle R diverges as $R \simeq r_0/\sin(\pi/n) \sim (r_0/\pi)n \to \infty$ and a regular polygon will naturally be stretched into a line (i.e., a stripe), as shown in Fig. 8. The minimal interaction energy for a regular polygon with a large number of hole dipoles is about

$$V^{d\text{-}d} \sim -2q^2 r_0^2 \sum_{kk'} \frac{1}{|\mathbf{r}_{kk'}|^2} \simeq -q^2 n. \tag{50}$$

When a dipole moves away from the line (a stripe), the finite energy cost $\Delta V^{d\text{-}d}$ will be

$$\Delta V^{d\text{-}d} \simeq -2q^2 r_0^2 \sum_{k'} \frac{1}{|\mathbf{r}_{k'}|^2} + 2q^2 r_0^2 \sum_{k} \frac{1}{|\mathbf{r}_k|^2} = \frac{q^2\pi^2}{24}(\delta r)^2, \tag{51}$$

where $\mathbf{r}_k = 2kr_0$ and $|\mathbf{r}_{k'}|^2 = |2\mathbf{r}_k|^2 + (\delta r)^2$. Thus the line shape configuration or stripe is stable against local perturbation.

In the above, the role of Coulomb interaction has not been considered. However, it is believed that the Coulomb interaction will stabilize the stripe, because in this configuration, most of the dipoles are far from each other, which also satisfies the demand of the repulsive Coulomb potential. Only the neighbor dipoles are as near to each other as possible. When the Coulomb interaction is taken into account, we expect the only extra effect is that the neighbor dipoles are repulsed to a longer distance. However, the stripe is stabilized.

It is easy to see that such a "stripe" of charge carriers is embedded in a domain wall of the AF background. To see this, we consider a stripe along the $\hat{x}$ axis composed of the hole dipoles of a size $|e| = r_0$ and spaced by $l = \alpha|\mathbf{e}|$. Far away from the $\hat{x}$ axis, the total spin twist summed from (14) is given by

$$\phi_i = \sum_k \phi_i^k = \sum_k \frac{e_x y_{ik}}{r_{ik}^2} \simeq \frac{\pi}{\alpha}\mathrm{sgn}(y_i), \tag{52}$$

when $|y_i| \gg r_0 \sim a$. Here $y_{ik} = y_i$ and $x_{ik} = lk + x_i$ according to the definition. Thus a phase shift is found across the stripe with

$$\Delta\phi = \phi_{y>0} - \phi_{y<0} = 2\frac{\pi}{\alpha}. \tag{53}$$

For the special case, $\alpha = 2$, the line becomes an antiphase domain wall,

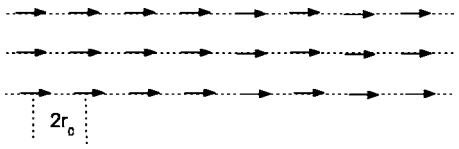

FIG. 9. When more holes are doped to occupy a certain concentration of the lattice grid, parallel lines are formed to make the stripe phase.

$$\Delta\phi = \phi_{y>0} - \phi_{y<0} = 2\frac{\pi}{\alpha} = \pi. \tag{54}$$

Thus, a stripe composed of hole dipoles is topologically an antiphase domain wall.

From Eq. (54), we can also understand physically the reason why the holes tend to arrange themselves into a straight line. When the hole dipoles are distributed randomly in the AF background, each dipole induces a spin twist as described by Eq. (14), which costs additional energy. But when the hole dipoles form a stripe, the total twist spins away from the domain wall will be canceled out such that the spin ordering on either side of the domain wall becomes unfrustrated, just as at half filling.

Yet there is a further advantage in the formation of the stripe, i.e., kinetic energy of can be gained by the holes. Recall that an isolated hole dipole cannot move freely as it is self-trapped in real space. But when the hole dipoles arrange themselves into a straight line, the individual holes actually may move freely along the stripe such that delocalization energy can be gained. This will correspond to a metallic stripe case.[19] However, when the Coulomb interaction is considered, it may prevent the holes from moving freely along the stripe, which turns it into an insulator. The property of the stripe may depend on the competition between the delocalization energy and the Coulomb interaction.

With a further increase of doping, more stripes will be formed as shown in Fig. 9. For any two stripes, when they are far from each other, without spin frustration inside the domain between them, they will not gain additional energy by being closer. Under long-range Coulomb repulsion, a uniform stripe phase will be stable against cluster formation. In this uniform stripe phase, the distances between two neighboring stripes are the same, which obviously is determined by the hole concentration. But when two stripes are so near that they are adjacent, it is shown by numerical calculations that they will attract each other and are bounded to form a ladderlike bond-centered stripe, which is supported by recent neutron scattering data.[10] The Coulomb interaction may prevent more stripes from being bounded. It should also be noticed that the recently found "checkerboard" pattern in the local density of states by scanning tunneling microscopy in the cuprate may display a new kind of charge-density-wave order.[30] Its possibility in the framework of the above mentioned dipole picture is under further exploration when the long-range Coulomb repulsion is considered more carefully.

IV. THE EFFECTS OF Zn IMPURITIES

As emphasized before, the stripe formation is intimately related to the self-localization of individual hole dipoles. We

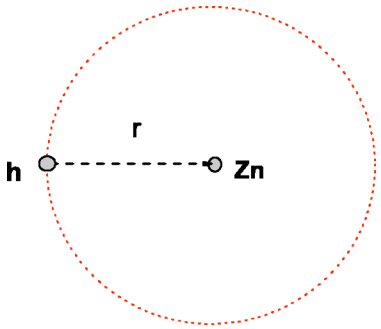

FIG. 10. (Color online) When a hole and a Zn^{2+} are doped into the AF background simultaneously, they would like to attract each other and form a Zn^{2+}-holon dipole. *H* denotes the holon, while Zn denotes the Zn^{2+}.

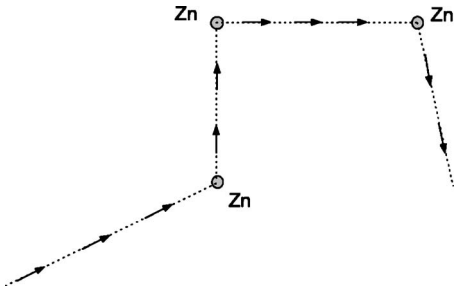

FIG. 11. A stripe in the presence of Zn^{2+}. The stripe has to pass the Zn^{2+}, and so is pinned.

also have mentioned that disorder or impurities in the system may have an "amplified" effect on localization.

In the following we discuss the effect of Zn impurities on hole dipoles as well as the stripe phase. It is well known that doped Zn atoms will be present in the form of Zn^{2+} with a closed-shell structure, substituting the Cu^{2+} sites in the CuO_2 planes of the cuprates. In the Zn^{2+} model, the site occupied by $t-J$ may be imposed by a boundary condition of an "empty" site where no electron or hole can remain at low energy.

Let us examine how a Zn impurity and a hole dipole will interact. Inside a hole dipole, those spins on a loop circling the center of the antimeron will have a 2π rotation in their polarization directions. As the radius of such a loop shrinks continuously to the antimeron core, the spin-polarization direction will change quickly and become uncertain at the core site. So a spin at the core site of the antimeron will just like a "defect" spin,[19] and the bonds that connect the core spin with its surrounding spins can be thus viewed to be effectively "cut off," resulting an energy increase of roughly $\sim 4J'$ (J' denotes the average superexchange energy for one bond). On the other hand, when a Zn^{2+} ion is doped and replaces a normal Cu^{2+} site, the bonds that used to connect such a Cu^{2+} with its surroundings are cut off with an energy cost of approximately $\sim 4J'$. But, if such a Zn^{2+} is to replace the Cu^{2+} at the core of the antimeron of a hole dipole, there will be no additional superexchange energy cost in breaking up those four bonds connected to the impurity site. Therefore, it will be energetically favorable for a hole dipole to be trapped by a Zn impurity. As shown in Fig. 10, a Zn impurity is located at the center of the antimeron. Experimentally, there is evidence[31] that doped holes are indeed trapped by Zn impurities.

According to the above discussions, a large number of Zn impurities will not favor stripe formation, for they tend to trap hole dipoles around themselves. A random distribution of the Zn leads to a random distribution of the hole dipoles. If the Zn concentration is very low, then a stripe is expected to be easily pinned by a Zn ion, and to be bent in order to pass several zinc ions, as shown in Fig. 11. From transport measurements[32] and also from muon-spin-relaxation measurements,[33] it is found that a small amount of Zn impurities is effective for the pinning. So we predict that Zn impurities are very effective in destroying the stripe phase at low doping.

V. CONCLUSION

In this paper, it is shown that in the framework of the phase-string model, each hole doped into a spin-ordered phase at low doping will act as a dipole which is self-trapped in real space. With the suppression of the kinetic energy, the dipole-dipole interaction between hole dipoles will dominate the low-energy physics in the absence of disorder or impurities. We demonstrated in detail how a few hole dipoles collapse into a stable configuration of the regular polygon, which turns into a stripe (stripes) in the thermodynamic limit. Consequently, we found that at a finite concentration of holes at low doping, a uniform stripe phase is highly competitive. The effects of impurities are also discussed. When a Zn^{2+} ion is doped into the system, it generally tends to trap a hole around itself to form a Zn^{2+}-holon dipole. As a result, the stripe will be pinned near the Zn^{2+} site. Furthermore, we predicted that a finite concentration of zincs ions can easily destroy a uniform stripe phase.

ACKNOWLEDGMENTS

We acknowledge stimulating discussions with Z. Y. Weng. This work is partially supported by NSFC Grants No. 90103021, No. 10247002, and No. 10204004. S.P.K. acknowledges support from Beijing Normal University.

*Electronic address: yangfan6278@sina.com.cn

[1] J. M. Tranquada, B. J. Sternlieb, J. D. Axe, Y. Nakamura, and S. Uchida, Nature (London) **375**, 561 (1995); J. M. Tranquada, J. D. Axe, N. Ichikawa, Y. Nakamura, S. Uchida, and B. Nachumi, Phys. Rev. B **54**, 7489 (1996).

[2] A. Bianconi, N. L. Saini, T. Rossetti, A. Lanzara, A. Perali, M. Missori, H. Oyanagi, H. Yamaguchi, Y. Nishihara, and D. H. Ha, Phys. Rev. B **54**, 12 018 (1996);M. V. Zimmermann, A.

Vigliante, T. Niemoeller, and N. Ichikawa, Europhys. Lett. **41**, 629 (1998).

[3] S. W. Cheong, G. Aeppli, T. E. Mason, H. Mook, S. M. Hayden, P. C. Canfield, Z. Fisk, K. N. Clausen, and J. L. Martinez, Phys. Rev. Lett. **67**, 1791 (1991); T. E. Mason, G. Aeppli, and H. A. Mook, *ibid.* **68**, 1414 (1992); K. Yamada, S. Wakimoto, G. Shirane, C. H. Lee, M. A. Kastner, S. Hosoya, M. Greven, Y. Endoh, and R. J. Birgeneau, *ibid.* **75**, 1626 (1995).

[4] Pengcheng Dai, H. A. Mook, and F. Dogan, Phys. Rev. Lett. **80**, 1738 (1998).

[5] F. C. Chou, F. Borsa, J. H. Cho, D. C. Johnston, A. Lascialfari, D. R. Torgeson, and J. Ziolo, Phys. Rev. Lett. **71**, 2323 (1993).

[6] F. Borsa, P. Carretta, J. H. Cho, F. C. Chou, Q. Hu, D. C. Johnston, A. Lascialfari, D. R. Torgeson, R. J. Gooding, N. M. Salem, and K. J. E. Vos, Phys. Rev. B **52**, 7334 (1995).

[7] J. H. Cho, F. C. Chou, and D. C. Johnston, Phys. Rev. Lett. **70**, 222 (1993).

[8] B. W. Statt, P. C. Hammel, Z. Fisk, S. C. W. Cheong, F. C. Chou D. C. Johnston, and J. E. Schirber, Phys. Rev. B **52**, 15 575 (1995); N. J. Curro, P. C. Hammel, B. J. Suh, M. Hucker, B. Buchner, U. Ammerahl, and A. Revcolevschi, Phys. Rev. Lett. **85**, 642 (2000).

[9] J. Zaanen and O. Gunnarsson, Phys. Rev. B **40**, R7391 (1989).

[10] S. R. White and D. J. Scalapino, Phys. Rev. Lett. **80**, 1272 (1998); **81**, 3227 (1998); M. E. J. Newman, C. Moore, and D. J. Watts, *ibid.* **84**, 3201 (2000); C. S. Hellberg and E. Manousakis, *ibid.* **83**, 132 (1999); **84**, 3022 (2000).

[11] J. Zaanen, Nature (London) **403**, 714 (2000); Science **286**, 251 (1999).

[12] G. Kotliar and J. Liu, Phys. Rev. B **38**, 5142 (1988).

[13] D. P. Arovas and A. Auerbach, Phys. Rev. B **38**, 316 (1988).

[14] B. I. Shraiman and E. D. Siggia, Phys. Rev. Lett. **62**, 1564 (1989); **61**, 467 (1988); C. Jayaprakash, H. R. Krishnamurthy, and Sanjoy Sarker, Phys. Rev. B **40**, 2610 (1989); D. Yoshioka, J. Phys. Soc. Jpn. **58**, 1516 (1989); C. L. Kane, P. A. Lee, T. K. Ng, B. Chakraborty, and N. Read, Phys. Rev. B **41**, 2653 (1990).

[15] Z. Y. Weng, D. N. Sheng, Y. C. Chen, and C. S. Ting, Phys. Rev. B **55**, 3894 (1997).

[16] W. Marshall, Proc. R. Soc. London, Ser. A **232**, 48 (1955).

[17] Z. Y. Weng, D. N. Sheng, and C. S. Ting, Phys. Rev. B **59**, 8943 (1999).

[18] Su-Peng Kou and Zheng-Yu Weng, Phys. Rev. Lett. **90**, 157003 (2003).

[19] S. P. Kou and Z. Y. Weng, Phys. Rev. B **67**, 115103 (2003).

[20] *Physical Properties of High Temperature Superconductors*, edited by D. M. Ginsberg (World Scientific, Singapore, 1989), Vol. 1, p. 154, Fig. 1.

[21] T. Thio, T. R. Thurston, N. W. Preyer, P. J. Picone, M. A. Kastner, H. P. Jenssen, D. R. Gabbe, C. Y. Chen, R. J. Birgeneau, and A. Aharony, Phys. Rev. B **38**, R905 (1988).

[22] I. Dzyaloshinskii, J. Phys. Chem. Solids **4**, 241 (1958); T. Moriya, Phys. Rev. **120**, 91 (1960).

[23] Amnon Aharony, R. J. Birgeneau, A. Coniglio, M. A. Kastner, and H. E. Stanley, Phys. Rev. Lett. **60**, 1330 (1988).

[24] V. Cherepanov, I. Ya. Korenblit, Amnon Aharony, and O. Entin-Wohlman, cond-mat/9808235 (unpublished).

[25] J. R. Schrieffer, X. G. Wen, and S. C. Zhang, Phys. Rev. B **39**, 11 663 (1989); D. M. Frenkel and W. Hanke, *ibid.* **42**, 6711 (1990).

[26] A. Singh and Z. Tesanovic, Phys. Rev. B **41**, 614 (1990); **41**, 11 457 (1990).

[27] A. L. Chernyshev, S. R. White, and A. H. Castro Neto, Phys. Rev. B **65**, 214527 (2002); A. L. Chernyshev, A. H. Castro Neto, and A. R. Bishop, Phys. Rev. Lett. **84**, 4922 (2000).

[28] Efstratios Manousakis, Nucl. Phys. B **20**, 689 (1991).

[29] B. P. Stojkovic, Z. G. Yu, A. R. Bishop, A. H. Castro Neto, and N. Gronbech-Jensen, Phys. Rev. Lett. **82**, 4679 (1999); Phys. Rev. B **62**, 4353 (2000).

[30] J. E. Hoffman, E. W. Hudson, K. M. Lang, V. Madhavan, H. Eisaki, S. Uchida, and J. C. Davis, Science **295**, 466 (2002); J. E. Hoffman, K. McElroy, D.-H. Lee, K. M Lang, H. Eisaki, S. Uchida, and J. C. Davis, *ibid.* **297**, 1148 (2002); C. Howald, H. Eisaki, N. Kaneko, M. Greven, and A. Kapitulnik, Phys. Rev. B **67**, 014533 (2003); M. Vershinin, Shashank Misra, S. Ono, Y. Abe, Yoichi Ando, and Ali Yazdani, Science **303**, 1995 (2004); H. C. Fu, J. C. Davis, and D.-H. Lee, cond-mat/0403001 (unpublished); P. W. Anderson, cond-mat/0406038 (unpublished); Han-Dong Chen, Oskar Vafek, Ali Yazdani, and Shou-Cheng Zhang, cond-mat/0402323 (unpublished).

[31] M. Hucker, V. Kataev, J. Pommer, J. Harass, A. Hosni, C. Pflitsch, R. Gross, and B. Buchner, Phys. Rev. B **59**, R725 (1999).

[32] Y. Koike, N. Kakinuma, M. Aoyama, T. Adachi, H. Sato, and T. Noji, J. Low Temp. Phys. **117**, 1157 (1999); Y. Koike, S. Takeuchi, Y. Hama, H. Sato, T. Adachi, and M. Kato, Physica C **282-287**, 1233 (1997); T. Adachi, I. Watanabe, S. Yairi, K. Takahashi, Y. Koike, and K. Nagamine, J. Low Temp. Phys. **131**, 843 (2003).

[33] I. Watanabe, and K. Nagamine, Physica B **259-261**, 544 (1999); I. Watanabe, T. Adachi, K. Takahashi, S. Yairi, Y. Koike, and K. Nagamine, Phys. Rev. B **65**, 180516(R) (2002); Physica B **326**, 305 (2003); T. Adachi, I. Watanabe, S. Yairi, K. Takahashi, Y. Koike, and K. Nagamine, J. Low Temp. Phys. **131**, 843 (2003); T. Adachi, S. Yairi, K. Takahashi, Y. Koike, I. Watanabe, and K. Nagamine, Phys. Rev. B **69**, 184507 (2004).